Determination of Load Composition Using Spectral Envelope Estimates

Steven B. Leeb, Member, IEEE Bernard C. Lesieutre, Member, IEEE Steven R. Shaw

Laboratory for Electromagnetic and Electronic Systems
Massachusetts Institute of Technology
Cambridge, MA 02139, USA

Abstract: *This paper describes the use of a harmonic sensor to estimate load composition from aggregate current waveforms. This sensor computes spectral envelopes that are short-term estimates of the fundamental and harmonic components of observed currents. With some limitations, this spectral information enables the accurate estimation of the number and type of physical components connected to sections of the electric power grid. This knowledge could allow a more precise control of steady-state and dynamic system behavior under all operating conditions. Preliminary experiments with a spectral envelope preprocessor have been conducted, and results from a hardware prototype are presented.*

I. Background

The spectral envelope preprocessor introduced in [1] and [2] computes short-term estimates of the fundamental and higher harmonic components of measured currents. In [1] and [3], load turn-on transients or "events" in spectral envelope estimates were used to develop a transient event detector for a nonintrusive load monitor (NILM). The NILM determines the operating schedule of the major electrical loads in a building from measurements made solely at the utility service entry. With the incorporation of the transient event detector, the applicability of the NILM is expanded to commercial and industrial environments where significant efforts, e.g., power factor correction and load balancing, are made to homogenize the steady-state behavior of different loads. The transient event detection algorithm permits the NILM to recognize individual loads by examining transients in measured spectral envelopes computed from the aggregated current waveforms available at the service entry.

The transient event detection algorithm is able to distinguish different electrical loads because the transient behavior of a typical load is strongly influenced by the physical task it performs. The turn-on transients associated with a fluorescent lamp and an induction motor, for example, are distinct because the physical tasks of igniting an illuminating arc and accelerating a rotor are fundamentally different. Distinctive transient profiles tend to persist even in loads which employ active waveshaping or power factor correction. The algorithm operates well even when many transients overlap to a significant degree.

At some high rate of event generation, the overlap of transients generally becomes so severe that the transient event detector is unable to distinguish individual load turn-on events. The peak tractable rate of event generation determines the extent to which the NILM with transient event detector can be "nonintrusive." A residence or moderate size commercial or industrial facility could generally be nonintrusively monitored with data from just the utility service entry. A very large facility or a substantial portion of the utility distribution network, on the other hand, probably could not be nonintrusively monitored to reveal detailed information about individual loads. These large sites typically have too many loads and too many events for the event detection algorithm to operate reliably. Smaller sections of these large target sites would have to be selected for successful nonintrusive transient monitoring with the event detector.

It may still be possible, however, to nonintrusively glean useful information about load composition at these larger sites. Several authors have observed interesting, potentially informative variations in power and harmonic content at different points in the utility distribution system (see [4], for example). This paper describes a technique for determining an estimate of load composition from measured, *steady-state* magnitudes of spectral envelopes.

The next two sections of this paper describe the theoretical foundation, implementation, and experimental results for a spectral envelope estimator. The following section describes an algorithm for estimating the significant load components from steady-state spectral envelopes. The technique is illustrated with results from a prototype, real-time event detector.

II. Spectral Envelope Estimation

The development of the spectral envelope estimator is stimulated by the generalized averaging techniques presented in [9] and by the short time Fourier transform

and Fourier series methods presented, for example, in [10] and [11] for speech processing and power systems simulation, respectively. With minor restrictions which cause no limitations in a practical power systems setting, a waveform $x(\tau)$ given as a function of τ may be described with arbitrary accuracy at time $\tau \in (t-T, t]$ by a Fourier series with *time-varying*, complex spectral coefficients $a_k(t)$ and $b_k(t)$:

$$x(t-T+s) = \sum_k a_k(t)\cos(k\frac{2\pi}{T}(t-T+s)) + \sum_k b_k(t)\sin(k\frac{2\pi}{T}(t-T+s)) \quad (1)$$

The variable k ranges over the set of non-negative integers; T is a real period of time, and $s \in (0, T]$.

The coefficients $a_k(t)$ may be found from the formula [9], [12]:

$$a_k(t) = \frac{2}{T}\int_0^T x(t-T+s)\cos(k\frac{2\pi}{T}(t-T+s))ds \quad (2)$$

Similarly, the coefficients $b_k(t)$ are computed by the formula:

$$b_k(t) = \frac{2}{T}\int_0^T x(t-T+s)\sin(k\frac{2\pi}{T}(t-T+s))ds \quad (3)$$

In practice, Eqns. 2 and 3 can be used to compute the evolution in time of the spectral coefficients $a_k(t)$ and $b_k(t)$ as an interval of interest of width T slides over the waveform x. The coefficients $a_k(t)$ and $b_k(t)$ as functions of time will be referred to as the *spectral envelopes* of x for the harmonic k.

Estimates of the spectral envelopes of current waveforms observed at the utility service entry of a building have proven remarkably useful for transient event detection in the NILM, for at least two reasons. First, even for waveforms x with substantial high frequency content, the frequency content of the spectral envelopes can be made relatively band-limited. As will be seen, this tends to ease the sample rate requirements on any single channel of the transient event detector. Second, in steady-state operation especially, estimates of the spectral envelopes serve as direct indicators of real and reactive power, as well as potentially undesirable harmonic content. Demonstrations of these claims follow.

For convenience, let

$$x_c(t) = \frac{2}{T}x(t)\cos(k\frac{2\pi}{T}t)$$

and

$$x_s(t) = \frac{2}{T}x(t)\sin(k\frac{2\pi}{T}t).$$

represent sinusoids modulated by the function x. Equations 2 and 3 are equivalent to convolving in time the integrands $x_c(t)$ and $x_s(t)$, respectively, with a rectangular pulse $p(t)$ with unit height extending from time 0 to time T, and may be written as

$$a_k(t) = x_c(t) \otimes p(t) \quad (4)$$

and

$$b_k(t) = x_s(t) \otimes p(t) \quad (5)$$

where the symbol $\otimes$ represents the convolution operator. In the frequency domain, the continuous time Fourier transform of the spectral envelope $a_k(t)$ is

$$A_k(f) = \int_{-\infty}^{\infty} a_k(t)e^{-j2\pi ft}dt.$$

From Eq. 4, the magnitude of $A_k(f)$ is equivalent to the product of the magnitudes of the functions $X_c(f)$, the Fourier transform of $x_c(t)$, and $P(f)$, the Fourier transform of the pulse $p(t)$. Similarly from Eq. 5, the magnitude of $B_k(f)$, the continuous time Fourier transform of $b_k(t)$, is the product of the magnitudes of $X_s(f)$, the transform of $x_s(t)$, and $P(f)$.

The effect of computing the spectral coefficients as an integral or average over the interval T is to attenuate the high frequency content of the spectral envelopes. Equivalently, the high frequency content of the spectral envelopes is attenuated by the (roughly) low-pass character of $P(f)$. The localization or high frequency attenuation in the frequency content of the spectral envelopes increases as the interval T increases in extent.

Each spectral coefficient indicates as a function of time the relative contribution of a sinusoid in the summations of Eq. 1. By varying the interval T it is possible to restrict to an essentially arbitrary degree the frequency content of the spectral envelopes, regardless of the harmonic k under consideration. A decomposition of even a relatively broad-band waveform x into spectral envelopes permits a trade-off, therefore, between sample rate per data channel and the number of data channels employed.

A second advantage of examining a waveform x in terms of spectral envelopes is the potential correspondence of the coefficients to familiar physical quantities in steady state. The term "steady state" is here taken to refer to a waveform or section of a waveform that is periodic. The interval T is presumed to be a positive integer multiple of the fundamental period of this waveform. Consider, for example, the situation in which the waveform x corresponds to an observed current waveform on a single phase of a utility system with a sinusoidal voltage waveform. For purposes of illustration, consider the voltage to be a cosine with angular frequency $2\pi/T$. Intuitively, Eqns. 2 and 3 compute the spectral coefficients by demodulating the periodic waveform x with an appropriate, harmonic sinusoid and low-pass filtering to preserve only the resulting lowest frequency components. For a periodic current waveform x with period T, the

Figure 1: Spectral Envelope Estimator

spectral coefficient $a_1(t)$ corresponds to a quantity that is proportional to the conventional definition of real or "time average" power [13]. Similarly, the coefficient $b_1(t)$ is proportional to reactive power. Higher order spectral coefficients correspond to in-phase and quadrature harmonic component content as in a conventional Fourier series decomposition of a periodic waveform.

While not necessarily essential, the ability to associate spectral envelopes with physical quantities is comforting when employing spectral envelopes as "fingerprints" for identifying loads. Variations in real and reactive power and harmonic content tend to be closely linked to the physical task or energy conversion process being performed by a load. Load classes that perform physically different tasks are therefore distinguishable based on their transient behavior [1]. Since the spectral envelopes are closely linked to telltale physical quantities, they serve as reliable metrics for identifying loads. Even when rates of event generation are so high that the transient event detection algorithm can not identify individual loads, it may still be possible to use steady-state or near steady-state spectral envelope characteristics to determine aspects of load composition.

III. Envelope Preprocessor

This section reviews the design of a hardware implementation of a spectral envelope preprocessor for use in the transient event detector. The preprocessor computes an estimate that approximates the spectral envelope integrals of Eqns. 2 and 3. Figure 1 illustrates the computation implemented in a single channel of the spectral envelope preprocessor. An observed current waveform $i(t)$, equivalent to the waveform x in the previous section, is mixed with a continuous time "staircase" or basis sinusoid. This basis sinusoid is constructed from discrete time samples, $v_b[n]$, of a desired, highly oversampled waveform. Analytically, these samples are reconstituted into a continuous time waveform by a zero order hold (ZOH). This process is line-locked by a phase-locked loop to the voltage waveform observed at the utility service entry, so that the reconstituted, basis sinusoid will exhibit a precise, desired phase with respect to the line voltage. The product of the current and basis sinusoid corresponds to a function such as $x_c(t)$ or $x_s(t)$ for a particular harmonic k, as described in the previous section. A multiplying digital-to-analog converter (MDAC) provides the ZOH and multiplication operations shown in Fig. 1. The product of a current and basis sinusoid is low-pass filtered (LPF) to yield an estimate of a particular spectral envelope for the current. A total of sixteen channels are available in the prototype for computing spectral envelopes.

In the prototype, a second order Butterworth filter with a breakpoint at 20 Hz is used on each channel to provide an estimate of the average or low-frequency component of each MDAC output. This low-pass filter, convenient from an implementation standpoint, is obviously not functionally identical to the windowed mean employed in Eqns. 2 and 3 to compute the spectral envelopes. For this reason, and because the basis waveforms are reconstructed with a (generally negligible) quantization error, the outputs of the prototype are *estimates* of the spectral envelopes. By varying the filter breakpoint, it is again possible to trade localization in time versus localization in frequency, as was possible in the previous section by varying the interval T. The slow roll-off of the output filters and slight offsets present in the prototype preprocessor will be seen to add small, high frequency ripple components to the spectral envelopes in the examples.

Five examples of the envelope estimator in operation will be considered here. In each case, the spectral envelopes will be observed to exhibit patterns created by the unique electrical, thermal, and mechanical processes that occur in each class of loads. Figure 2, for example, shows the measured current waveform and four associated spectral envelopes estimated by the preprocessor during the turn-on transient of a bank of instant start fluorescent lamps. All five waveforms were captured with a digital storage oscilloscope. The top trace in Fig. 2 shows the current into the lamps during the transient and in steady state. The remaining four traces, labeled $a1$, $b1$, $a3$, and $b3$, correspond to the envelope estimates of real power, reactive power, in-phase third harmonic content, and quadrature third harmonic content, respectively. In the transient event detector described in [3], the characteristic patterns in the spectral envelopes dur-

ing the turn-on transient would be used to recognize the turn-on event of the instant start lamps. Where rates of event generation are very high, the transient event detector will be unable to recognize the event; in the following sections of this paper, we will consider the use of the *steady-state* spectral envelope values to assist in determining load composition.

Figure 3 shows the current and four spectral envelopes on one phase during the turn-on transient of a three phase induction motor. While the rotor is accelerating to steady-state speed, the motor draws a relatively large current, as shown in the top trace of Fig. 3. Around 0.3 seconds into the transient, the rotor has reached its nominal velocity and the input current tapers to its steady-state level. The trace labeled a_1 in Fig. 3 again corresponds to the slow envelope of real power. The trace labeled b_1 corresponds to the slow envelope of "reactive power." As might be expected, the induction motor does not exhibit unity power factor, and the magnitude of the b_1 trace in steady state is substantial relative to the magnitude of the a_1 trace. Also, as would be expected for a balanced three phase load, the induction motor draws no third harmonic components.

Figure 4 shows the turn-on transient for the current and spectral envelopes of a bank of rapid start fluorescent lamps.

Figure 5 shows the current and envelopes during the turn-on transient of a personal computer (PC). The switching power supply inside the computer initially draws a few large pulses of current as the internal bus capacitor charges from the line through a full bridge rectifier. When the capacitor has built up a substantial stored charge, the current waveform becomes "spikey" as charging begins to occur only near the peaks in the magnitude of the line voltage waveform. Approximately 0.18 seconds into the transient, the computer monitor turns on, increasing the total steady-state current drawn by the computer and monitor. The fourth trace, labeled a_3, is computed by mixing the current with a sinusoid with the same phase but three times the frequency of the line voltage. This spectral envelope indicates in-phase third harmonic content. As might be intuitively expected from examining the "spikey" line current waveform, the computer draws a substantial third harmonic current.

Finally, Fig. 6 shows the current and four spectral envelopes measured during the turn-on transient of a bank of incandescent lamps.

It is our goal to use known spectral envelopes of typical loads to estimate load composition from the measured spectral envelope of an aggregate load. We assume, for the purposes of this paper, that our knowledge is limited to steady-state spectral envelope measurements of dominant load types and steady-state or quasi-steady-state measurements of the aggregate load. There is additional, potentially useful information for load disaggregation, and modified monitoring techniques that will aid in our pursuit of more detailed load composition estimates and models. We discuss these in Section V. In this paper we focus on the mathematical decomposition aspects of our approach.

Table 1: Individual Load Characteristics

	Instant Starts β_1	0.25 HP Motor β_2	Rapid Starts β_3	PC β_4	Incandescent β_5
a_1	0.351	0.054	0.307	0.106	0.429
b_1	0.003	0.088	-0.044	-0.006	-0.002
a_3	-0.066	-0.000	-0.005	0.092	-0.006
b_3	0.063	-0.004	-0.010	-0.013	0.004

IV. Identifying Load Components

In this section we present a method for identifying the amount of certain classes of loads in an aggregate load. This is achieved by representing the load components and measured aggregate loads in a linear vector space whose dimensions correspond to the amplitudes of the spectral envelopes. In this space we can employ linear techniques to decompose the total observed load into some of the important load components. We emphasize the theoretical and practical limitations of this approach and present results demonstrating its potential.

The basis approach

We represent each load's steady-state operating characteristic as a vector of spectral envelope values. The loads in our study and their characteristics are listed in Table 1. For instance, the vector describing the incandescent lights is given in the last column,

$$\beta_5 \;=\; [0.429 \;-0.002 \;-0.006 \;0.004]\,.^T \qquad (6)$$

In steady state, the incandescent lamp is essentially a resistor, and draws only real power. This is indicated in the basis vector β_5 by the negligible reactive and third harmonic components.

Given an aggregate load measurement we attempt to determine how much of each load type is present in the aggregate. To aid in this we define the "basis matrix"

$$\begin{aligned} B &= [\beta_1\ \beta_2\ \beta_3\ \beta_4\ \beta_5\ ] \\ &= \begin{bmatrix} 0.351 & 0.054 & 0.307 & 0.106 & 0.429 \\ 0.003 & 0.088 & -0.044 & -0.006 & -0.002 \\ -0.066 & -0.000 & -0.005 & 0.092 & -0.006 \\ 0.063 & -0.004 & -0.010 & -0.013 & 0.004 \end{bmatrix} \end{aligned} \qquad (7)$$

The amount of each load component is determined from the solution of

$$Bx = \beta_{obs} \quad (8)$$

where x is the amount of each load type in the observed aggregate vector of spectral envelope amplitudes, β_{obs}. The solution of this linear algebra problem depends on the properties of the basis matrix B and the observed vector β_{obs}.

Assuming the basis matrix $B \in R^{mxn}$ is constructed to have full rank, Equation (7) is

- *overconstrained* if $m > n$ and typically will not have a solution;
- *underconstrained* if $m < n$ and typically will have an infinite number of solutions related through the nullspace of B;
- *invertible* and exhibits a unique solution if $m = n$.

(Other possibilities exist if matrix B is not full rank, but are not pursued here.)

From a mathematical viewpoint one might expect that the square matrix is ideal. This is not the case. We neither expect to be able to account for every possible load, nor expect that all loads will have independently distinguishable basis vectors. A full-rank, square matrix B leaves no room for error or uncertainty. The overconstrained case is better. The measurement, β_{obs} will not typically be represented exactly by the basis vectors; a least-squares estimate will give a best fit. The error accounts for unknown loads. This case occurs when the number of nontrivial spectral components is greater that the number of significant load types.

In practice, we encounter the underconstrained case. There are a large number of interesting loads which are not uniquely identifiable from their basis vectors. In our study, we made measurements of first and third harmonics on five different types of loads. The basis matrix B is a four-by-five matrix.

We might force the problem to be overconstrained if we know that certain loads are not present or are negligible. In general, one cannot expect that forcing the underconstrained problem to be overconstrained will give accurate results in the variables of interest because the load basis vectors are not orthogonal. Loads that have significant presence but are not accounted for in the basis will not appear in the error, but will be reflected in the estimate of other load components. For example, suppose we are only interested in the portion of the load corresponding to instant start lamps. We might simply pose the problem as

$$\beta_1 x = \beta_{obs}, \quad (9)$$

where x here represents the scalar number of instant start lamps. Now suppose the load actually consists of only rapid start lamps, $\beta_{obs} = \beta_3$. A least squares analysis does not yield $x = 0$, indicating no instant start lamps; rather, it will falsely indicate a large portion of instant start lamps. This is a direct result of not having orthogonal load basis vectors.

This observation leads to an approach by which one can identify the components of certain loads which are distinguished by a having a significant component in a direction orthogonal to the other loads.

The orthogonal component approach

Even in the underconstrained case, a load could be distinguished if it has a component that is orthogonal to the space spanned by the remaining load basis vectors (excluding the load of interest). While it is unlikely that this will occur exactly in a numerical sense due to uncertainties, from a practical perspective this could occur and is not accidental. Loads have different physical characteristics because of real, physical differences in how energy is processed.

Note that the loads described by vectors β_2, β_3, and β_5 in Table 1 are practically limited to real and reactive components in steady state. Any third harmonic content in the aggregate steady-state measurement must arise from a load other than these three.

For example, we can now estimate the portion of the load that comes from instant start lamps. The four-by-four matrix of the load vectors excluding the instant starts and neglecting third harmonics where appropriate is

$$\begin{aligned} B_R &= [\beta_2\ \beta_3\ \beta_4\ \beta_5] \\ &= \begin{bmatrix} 0.054 & 0.307 & 0.106 & 0.429 \\ 0.088 & -0.044 & -0.006 & -0.002 \\ 0.000 & 0.000 & 0.092 & 0.000 \\ 0.000 & 0.000 & -0.013 & 0.000 \end{bmatrix} \end{aligned} \quad (10)$$

and has $rank = 3$. The nullspace of B_R^T is one dimensional. It is the orthogonal complement of the space spanned by the columns of B_R and in this case can be represented by the vector

$$\beta_n = [0.000\ 0.000\ -0.013\ -0.092]^T \quad (11)$$

The instant start lamp has a component in the direction of this nullspace vector. With proper scaling, the component of the aggregate load corresponding to the instant start lamps can be found by projecting the observed vector onto the nullspace. The component of the observed vector in the nullspace is proportional to the quantity of instant start lamps in the aggregate load.

The proper scaling is found by projecting β_1 onto β_n. The vector p_n defined by

$$p_n = \beta_n / (\beta_n^T \beta_1) \quad (12)$$

Table 2: Aggregate Load Characteristics

	A	B
a_1	0.8690	1.1108
b_1	0.0614	0.0539
a_3	0.0021	-0.0056
b_3	0.0498	0.0536

Table 3: Instant Start Lamp Component

	Estimate	Error
Load A	0.938	6.2%
Load B	0.990	1.0%

can be used directly with the aggregate load measurement to determine the number of instant start lamps,

$$lamps \quad = \quad p_n^T \beta_{obs} \tag{13}$$

This is demonstrated by the examples presented next.

Examples

We examine two aggregate loads:

A. This load consists of one set of instant start lamps, a PC, a 0.25 HP three-phase motor, and a set of incandescent lights (four 100W bulbs).

B. This load is identical to Load A with an additional 200W incandescent bulb.

The measured amplitudes of the steady-state spectral envelopes of these aggregate loads are presented in Table 2. The estimate of the number of instant start lamps computed with Equation 13, and the error in the estimate, are listed in Table 3.

The measurements were made in the presence of noise and uncertainties. This is evident since the sum of the individual basis vectors comprising the aggregate load differ from the measured aggregate. The errors of 6.2% and 1% are encouraging. With more accurate sensors we expect that these errors will be reduced.

V. Conclusions

The Nonintrusive Load Monitor accurately identifies loads through transients in observed spectral envelopes. At some point we expect that individual load transients will occur too frequently and at levels too small to be distinguished from noise in the system. At this point, we wish to determine if the quasi-steady-state spectral envelopes can be used to provide an estimate of load composition. This initial study indicates that the contribution of certain load types having a physical operating characteristic that uniquely distinguishes them from the other loads present can be disaggregated from an observed measurement. In our example the instant start lamps fit this description. We proposed a method for obtaining this estimate. We emphasize that the key step is to identify the portion of a vector of interest that is orthogonal to all other load basis vectors.

We may also, for example, use the following additional information to gain a better estimate of load composition. Knowledge of the types of loads that are expected to be dominant and those that will not be present will reduce the number of load basis vectors that need be considered. Also, since load behavior is governed by physical properties we expect that measurements of higher harmonics will yield more information. It is likely that some power electronic loads, for example, will be distinguishable in the higher harmonics. We could also use the constraint that loads appear in positive amounts.

Finally, temporal changes could be used to estimate load composition. By monitoring incremental changes, we could estimate changes in the aggregate. In the previous example, the difference between Loads A and B was the presence of an additional 200 W incandescent bulb. The difference between the measured characteristics is

$$\beta_{diff} \quad = \quad [0.242 \ -0.008 \ -0.010 \ 0.004]^T \tag{14}$$

which corresponds to a real power load. By examining Table 1 we can see from the difference that an incandescent load was added to the aggregate. Knowing that the basis vector β_5 comes from four 100 W bulbs, we may further estimate an increase of 200 W. We emphasize that this information cannot be deduced directly from the absolute measurement but is concluded from an incremental measurement.

The approach to determining particular load components by first identifying the distinguishing characteristic of these loads is theoretically sound and will accurately capture certain loads. The overall usefulness of this method will depend upon the number of loads that can be distinguished. We could, for example, try to capture a subset of all loads, such as the component of the total load consisting of all power electronic devices.

Acknowledgements

The authors gratefully acknowledge the valuable advice and support of Professors George Verghese and Chris DeMarco, Dr. Richard Tabors, Frank Porretto, and Laurence Carmichael. SBL and SRS were funded in part by ESEERCo. and EPRI. BCL was sponsored in part by the National Science Foundation under grant ECS-9409676. Essential hardware for this project was made available

through generous donations from the Intel Corporation and Tektronix.

References

[1] Leeb, S.B., "A Conjoint Pattern Recognition Approach to Nonintrusive Load Monitoring," M.I.T. Ph.D. Dissertation, Department of Electrical Engineering and Computer Science, February 1993.

[2] Leeb, S.B., S.R. Shaw, "Harmonic Estimates for Transient Event Detection," *Universities Power Engineering Conference,* Galway, Ireland, September 1994.

[3] Leeb, S.B., S.R. Shaw, J.L. Kirtley, Jr., "Transient Event Detection in Spectral Envelope Estimates for Nonintrusive Load Monitoring," *IEEE PES Winter Meeting*, Paper 95 WM 042-2-PWRD New York, NY, January, 1995.

[4] Emanuel, A.E., J.A. Orr, D. Cyganski, and E.M. Gulachenski, "A Survey of Harmonic Voltages and Currents at the Customer's Bus," *IEEE Transactions on Power Delivery*, Vol. 8, No. 1., pp. 411–421, January 1993.

[5] Kern, E.C., "Meter Sorts Load for Appliance Use," *Electrical World*, p. 75, April 1986.

[6] Hart, G.W., "Nonintrusive Appliance Load Monitoring," *Proceedings of the IEEE*, Vol. 80, No. 12, pp. 1870–1891, December 1992.

[7] Leeb, S.B., and J.L. Kirtley, Jr., "A Multiresolution Transient Event Detector for Nonintrusive Load Monitoring," *International Conference on Industrial Electronics, Control, and Instrumentation 1993*, Maui, Hawaii, pp. 354-359, November 1993.

[8] Leeb, S.B., and J.L. Kirtley, Jr., "A Transient Event Detector for Nonintrusive Load Monitoring," U.S. Patent Application, filed December 1993.

[9] Sanders, S.R., J.M. Noworolski, X.Z. Liu, and G.C. Verghese, "Generalized Averaging Method for Power Conversion Circuits," *IEEE Transactions on Power Electronic Circuits,*, Vol. 6, No.2, pp. 251–259, April 1991.

[10] Oppenheim, A.V., *Applications of Digital Signal Processing*, Prentice-Hall, Inc., Engelwood Cliffs, New Jersey, pp. 117–168.

[11] DeMarco, C.L., and G.C. Verghese, "Bringing Phasor Dyanamics into the Power System Load Flow," *North American Power Symposium*, 1993.

[12] Siebert, W.M., *Circuits, Signals, and Systems*, McGraw–Hill, New York, New York, p. 370.

[13] Kirtley, Jr., J.L., "AC Power Flow in Linear Networks," M.I.T. 6.061 Supplementary Notes 2, June 1987.

[14] Slemon, G.R., *Magnetoelectric Devices: Transducers, Transformers, and Machines*, John–Wiley and Sons, 1966.

[15] Basseville, M., and A. Benveniste, *Detection of Abrupt Changes in Signals and Dynamical Systems*, Springer–Verlag, 1980.

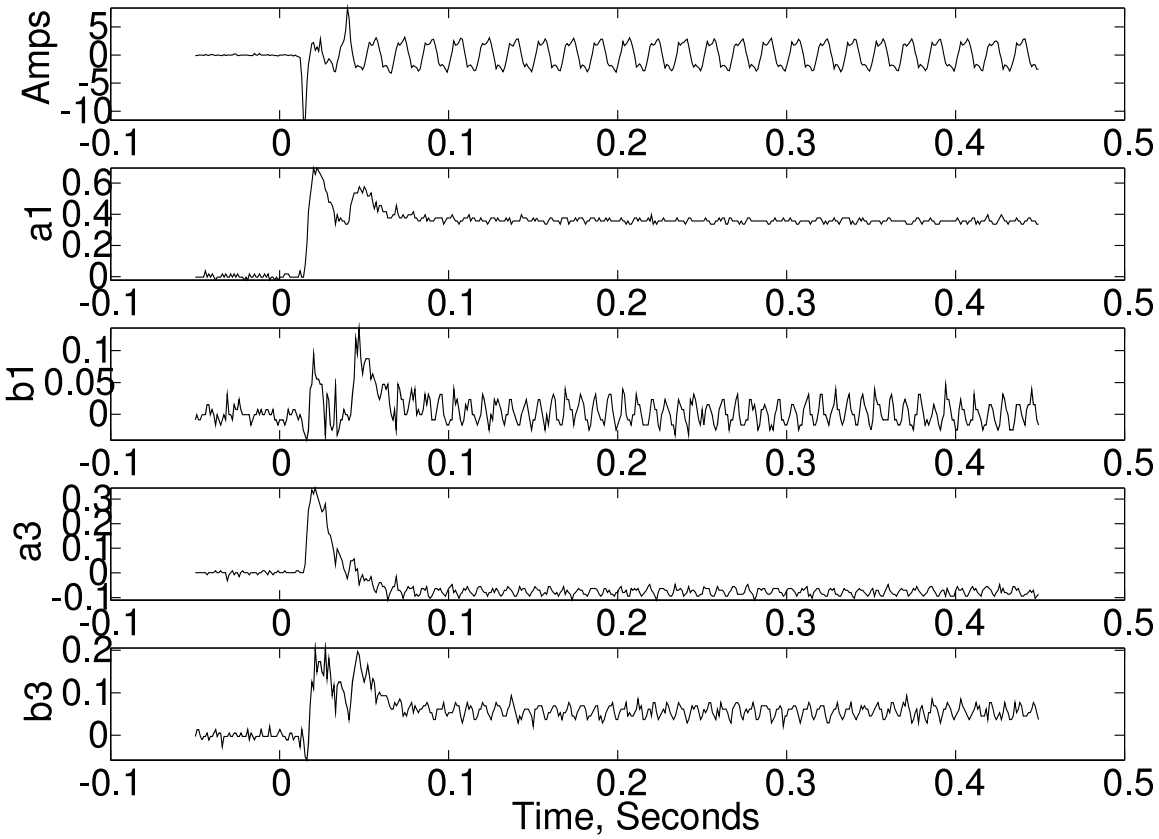

Figure 2: Instant Start Fluorescents: Spectral Envelopes

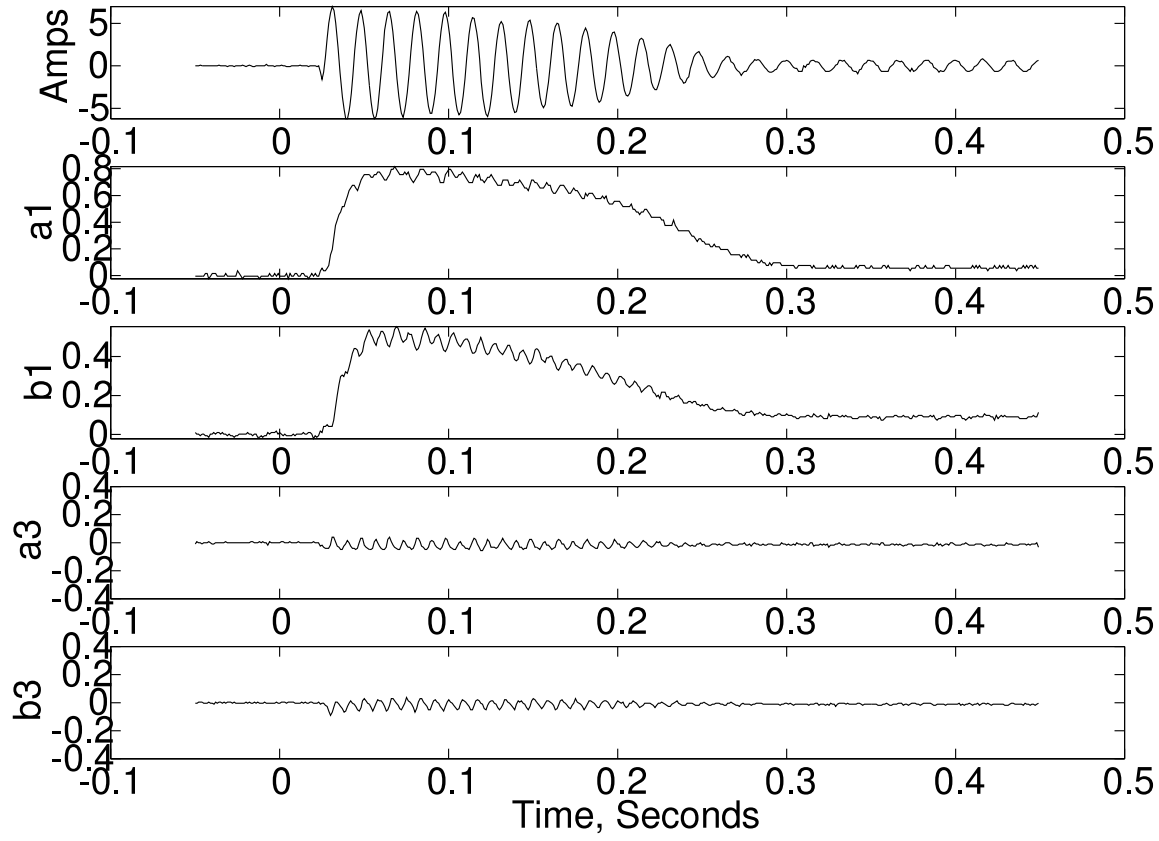

Figure 3: Induction Motor: Spectral Envelopes

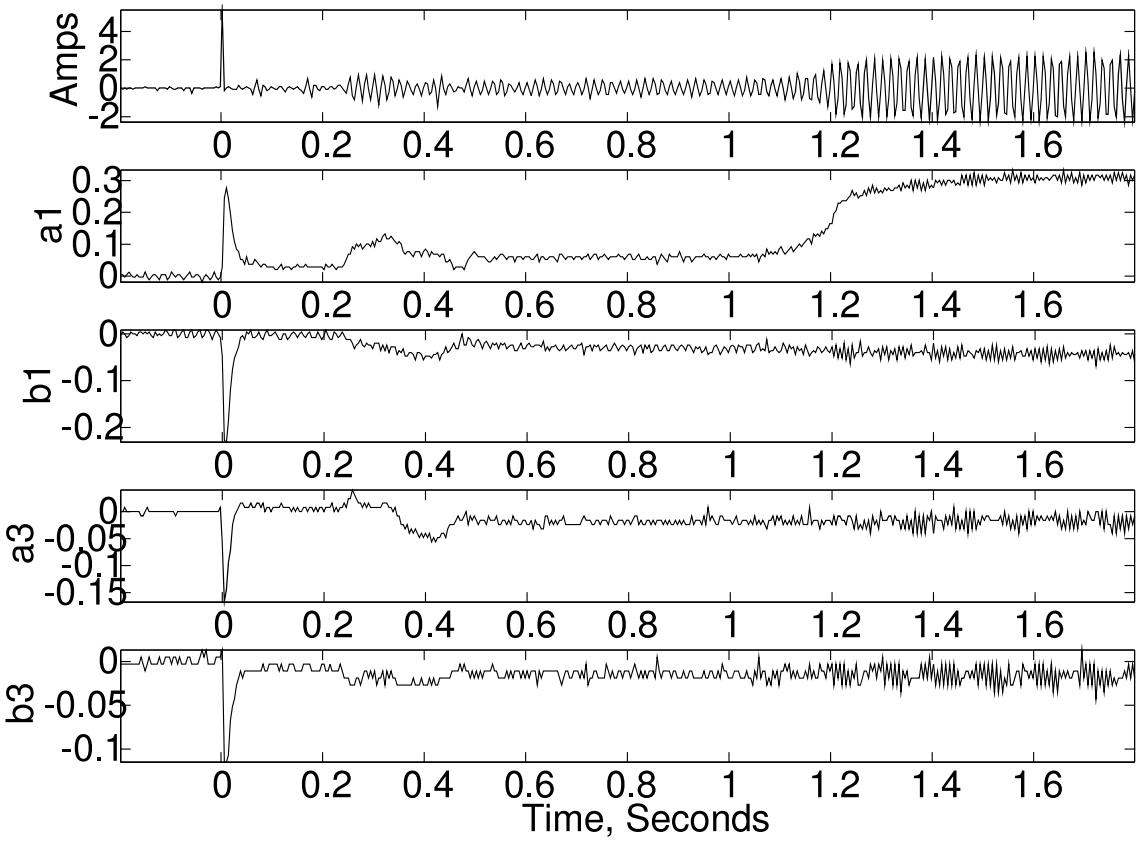

Figure 4: Rapid Start Fluorescents: Spectral Envelopes

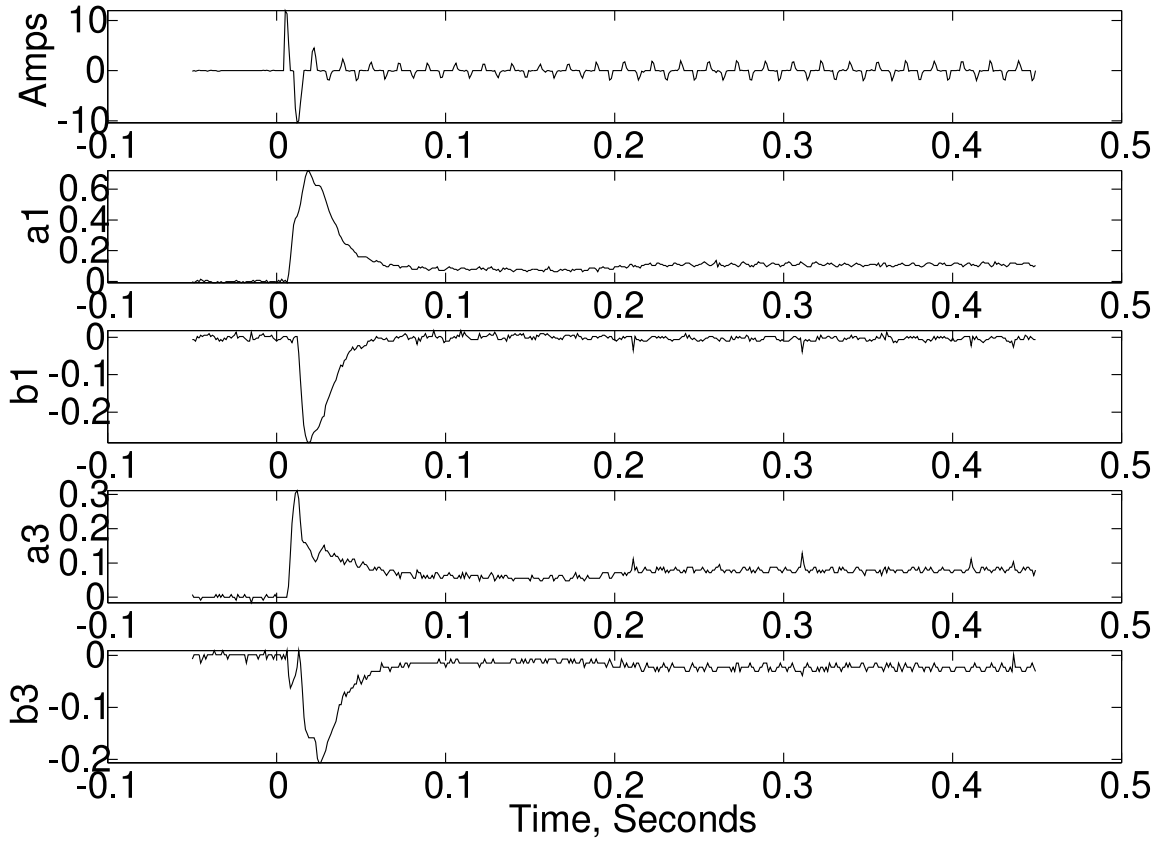

Figure 5: Personal Computer: Spectral Envelopes

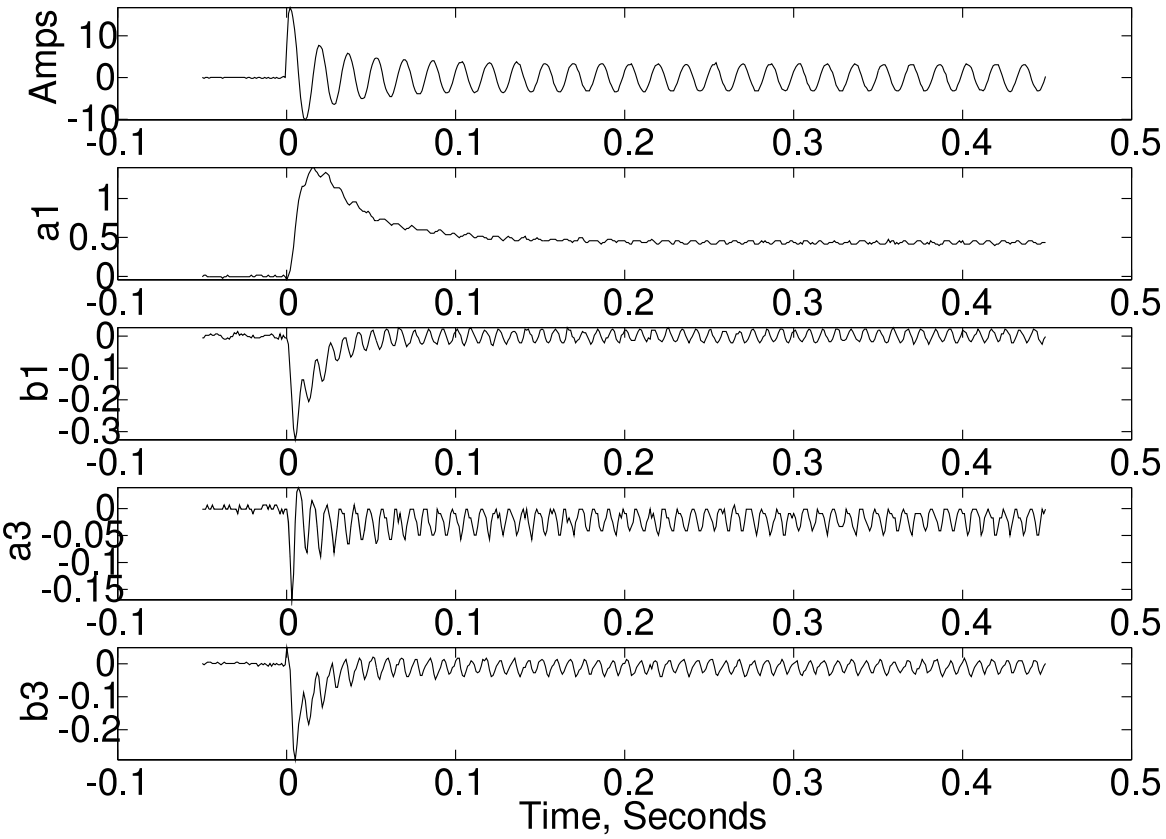

Figure 6: Incandescent Lamps: Spectral Envelopes